Photoswitchable catalysis using organometallic complexes.

Zoraida Freixa*[a, b]

Received 00th January 20xx,
Accepted 00th January 20xx

DOI: 10.1039/x0xx00000x

This review describes the state of the art in photoswitchable organometallic catalysis, underlining the importance of ligand design. The implementation of spatio-temporal control on known catalytic processes has been appealing to several researchers for a long time. Even though the area is still in its infancy, the diversity of the existing examples shows that there are plenty possibilities in terms of the photochromic actuator of choice, and on the expected effect of the photochemical transformation on the catalytic process. The pioneering examples discussed here are, in many cases, just basic models far from efficient. However, they suffice to envisage the magnitude of the space that remains unexplored, letting us foresee that exciting innovations are awaiting.

1. Introduction

Homogeneous catalysis using organometallic‡ complexes is a mature area of research.[1] The progress in the field was driven by the continuous improvement of the efficiency and selectivity of organic transformations while addressing engineering, post-reaction purification, and environmental aspects.[2]

Homogeneous catalysis depends on the use of specific ligands coordinated to a metallic core to modify the catalyst activity and/or selectivity through fine-tuning their steric (morphology) or electronic properties.[3] Ligands can also influence the solvent-affinity of the complexes allowing them to be applied in biphasic, aqueous or unconventional media (such as supercritical CO_2, fluorinated solvents, ionic liquids, etc.), or enabling their immobilization on solid or macromolecular supports. Nowadays, one can say that an educated choice of the appropriate metal, combined with the right ligand, not only facilitates that many known organic reactions occur more efficiently and selectively, but it also opens the access to new transformations, enlarging the modern organic synthesis tool kit.

Some of the latest advances in the field are directed to the integration actuators and control systems into known functional molecular catalysts. They are based on stimuli-responsive organometallic complexes, able to toggle between states with different intrinsic catalytic properties.[2, 4] Traditional molecular catalysts are static entities with well-defined properties and fixed catalytic functions, dictated by the initial reaction conditions. In contrast, these catalytic molecular machines are expected to perform (multiple) stimuli-controlled catalytic tasks, mimicking the mode of action observed in many enzymes. The implementation of such controlled functional diversity opens new dimensions into the homogeneous catalysis scenario, as it allows for an external intervention during the development of the chemical process. Prospective applications range from the "simple" on/off control of the catalytic activity, to time- and/or space-defined liberation of specific products, eventually form a reservoir of mixed substrates, permitting sequential or parallel reactions to occur in a controlled manner. These systems will permit intricate reaction sequences to occur in a single vessel through the combination of orthogonally controlled single steps, mimicking the spatio-temporal regulation of complex biological functions encountered in nature.

Polymer science is the field in which one encounters most of the practical examples. Remotely controlled systems that can produce sequence-controlled multiblock structures have been implemented by regulating the exposure to different orthogonal stimuli.[5]

Concerning the input signal, light seems the most appropriate stimulus to control the state of the catalyst. In contrast to chemical triggers, it perturbs the system in a non-invasive and non-cumulative manner. Additionally, it presents the advantage that it can be dosed with high spatio-temporal resolution and the proper modulation of its intensity and wavelength offers an additional control on the photochemical actuation.

Following the lessons learned from conventional homogeneous catalysis, ligands design is a must in the blueprint for success in the development of photo-controlled catalysts. They must contain the light-responsive actuator (a photochromic unit selected from the well-known pool of organic photoswitches). The way the actuator interferes with the chemical reactivity of the catalyst must be carefully addressed. Its effectivity depends on a precise identification of the key properties of the ligand that affect the different aspects of the catalytic event, to maximize its difference between the switching states.

[a] *Department of Applied Chemistry, University of the Basque Country (UPV-EHU), 20018, San Sebastián, Spain.*
[b] *IKERBASQUE, Basque Foundation for Science, Bilbao, 48013, Spain.*
e-mail: Zoraida_freixa@ehu.eus.

The intrinsic properties of the photochrome must be also optimized. Ideally, it should show a nearly quantitative photochemical conversion (high concentration of one or other isomer in the photo-stationary state, PSS), reversibility (either photochemical or thermal), thermal stability of the metastable isomer, high resistance to fatigue, a fast response (ideally faster than the chemical process itself), and resistance to decomposition.[5d, 6] Additionally, irradiation must be orthogonal to the catalytic chemical transformation, which must be confirmed experimentally using analog systems containing non-photochromic ligands.

Several existing reviews and research papers include descriptions of the development of photoswitchable homogeneous catalysis from diverse perspectives.[2, 4, 5c, 6-7] This contribution focusses on homogeneous catalytic reactions with organometallic compounds regulated by photoresponsive ligands, underlining the rationale behind the ligand design and covering from the pioneering examples to the most recent developments. Other light-mediated catalytic processes in which light is used as source of energy for the catalytic reaction (photoredox catalysis) or in which an irreversible transformation on the organometallic complex to form the actual catalytic species occurs due to light absorption (photocaged catalysis), will not be discussed here.

Selected examples of photoswitchable ligands, not necessarily synthesized for catalytic purposes, have been mentioned in the last section. They are intended to serve as inspiration for future developments.

2. **Photoswitchable activity.**

When thinking about photoswitchable catalysis the most evident idea is to address the activity of the catalyst through irradiation, being the binary switch (on/off) the ideal situation (Figure 1). Many practical applications can be envisaged from such “simple” control: the design of complex chemical systems containing “dormant” catalysts to activate specific chemical processes *ad-lib*, the implementation of synchronized sequential processes through mixtures of orthogonally-controlled catalysts with complementary reactivities, or space-/time-controlled delivery of products are just some of the many appealing possibilities.

Several authors constructed prototypes of catalysts with photoswitchable activity, targeting particular changes on the ligand through the switch of the actuator. The design was usually inspired by the learning on the ligand properties that most influence de catalytic activity for each specific process. The existing examples are described here, based on the light-induced modification pursued.

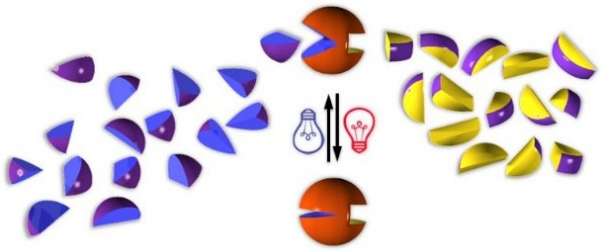

Figure 1. Photoswitchable catalytic activity.

Photo-induced ligand coordination/extrusion.

Ligand photolysis to generate an active catalyst that facilitates a thermal reaction is a recurrent mechanism to activate certain inner-sphere catalytic processes. Representative examples concern photochemical extrusion of CO,[8] acetylacetonate,[9] nitrile[10] or arene,[11] or the displacement of a coordinated acetylacetonate in the presence of a photo-acid generator.[12] All of them were successfully applied as the initiation mechanism in several olefin metathesis reactions,[7f, 7i, 13] among other catalytic processes.[9, 14]

More recently, the photogeneration of free ligands that coordinate inactive precatalysts has also been applied as the activation mechanism in ring-opening metathesis polymerization reactions (ROMP).[15]

Both, light-induced ligand extrusion and coordination proved effective as photoinitiation mechanisms. However, they lack the reversibility required for an externally-regulated system, falling under the category of photocaged catalysis.

As it is well-known, the coordination properties of a ligand are determined by a balance between their steric and electronic properties. Therefore, if properly designed, photochromic ligands can be used as actuators in certain catalytic processes in which ligand coordination/release is required to trigger the catalytic event.

In 1999, in a pioneering example, Inoue developed a photo-controlled catalytic system for the chemical fixation of CO_2 based on a photo-controlled ligand coordination/extrusion.[16] This early example was based on the activating effect of N-based basic ligands to promote the carbonation of epoxides using a (tetraphenylporphyrinato)aluminum alkoxide precatalyst (Figure 2).[17] It was already established that coordination of the basic ligand produced a change in the aluminum coordination environment from square pyramidal to square planar, drifting the alkoxide closer to the porphyrin plane. These changes resulted in an enhanced reactivity towards CO_2, and also a better stability of the formed aluminum-carbonate. It further reacted with an epoxide to form the cyclic carbonate and regenerate the active catalyst.[17] Additionally, they observed that the coordination of 2-stilbazole ligands on the axial position of metalloporphyrins was a reversible photo-controlled process.[18] Their strategy was to unify both findings designing a photochromic 3,5-di-*t*-butyl-2-stilbazole ligand (**1**). In the thermodynamically stable *E* form, steric repulsion between the bulky *tert*-butyl groups and the

porphyrin ring hampered its coordination to the Al(III) center. Under UV-irradiation, the ligand isomerized to the *Z* configuration, which facilitated its coordination to the axial position of the aluminum-porphyrin.

Dark reactions using isolated ***Z*-1** and ***E*-1** isomers of the 2-stilbazole ligand reflected the activating effect of the coordinated *Z*-ligand (28% vs. 2% conversion after 18 h at 25 °C, respectively) and the reversibility of the process was confirmed by switching between the ON and OFF states of the catalyst during a single catalytic run.

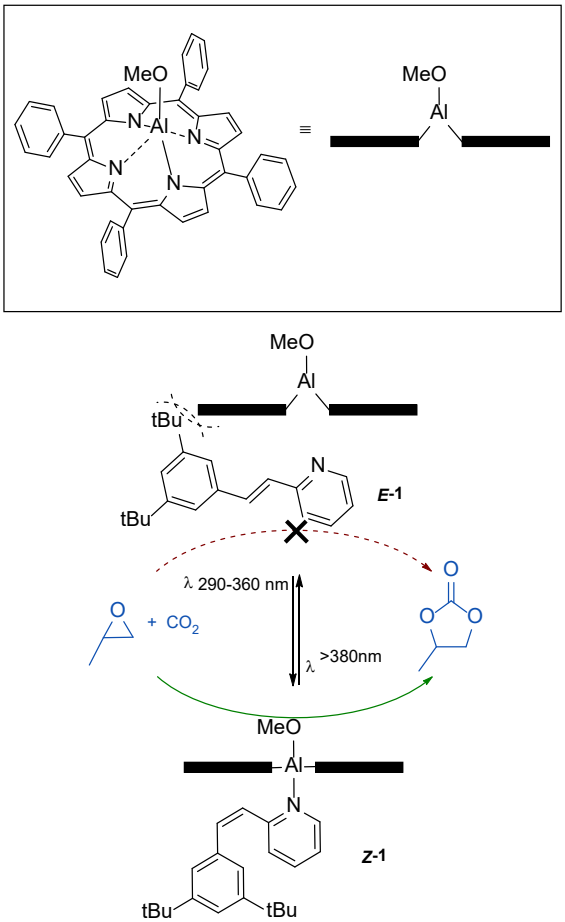

Figure 2. Photoswitchable catalyst for the carbonation of epoxides. Green-continuous and red-dashed arrows represent operative and non-operative processes, respectively.

From a conceptual point of view, the design of a photochromic ligand able to control the activity of a catalyst by forcing the extrusion of one of the coordinated ligands (opening a vacant site ready to activate the substrate) seems a relatively simple approach. Surprisingly, no functional examples appeared up to date. The only system showing a related light-induced ligand ejection mechanism was described by Bogliotti and Xie in 2016.[19] Quantitative photorelease of a coordinated triphenylphosphine ligand from a cationic arene ruthenium(II) complex (**2**) was observed through *Z*-*E* isomerization of an *ortho*-tosylamide azobenzene coordinated ligand,[20] helped by solvent coordination (Scheme 1). Unusually, in this case, the actual catalyst was the liberated phosphine rather than the ruthenium species. This example demonstrates that constructing a light-controlled ligand-ejection mechanism is a feasible approach. However, the reversibility of the process is a tricky issue that needs further development. Even though the photochromic actuator recovers the "coordination-allowing" state, the ejected ligand will compete with large quantities of substrate and solvent for the available coordination site.

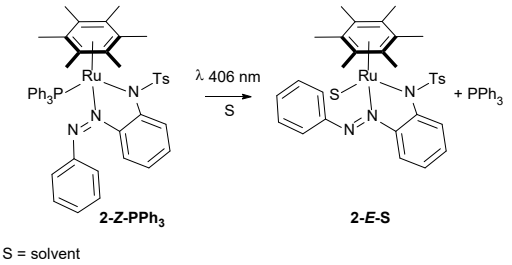

Scheme 1. Photocaged phosphine catalyst.

Photo-modulation of the steric and/or electronic properties of coordinated ligands.

The activity of an organometallic catalyst is strongly influenced by the steric and electronic properties of the coordinated ligands.[1, 3] Taking into account the evident geometrical changes that some of the well-known organic molecular switches experience upon light irradiation, the use of photoinduced morphological changes on the ligand to modify the catalyst activity seems a straightforward approach.

In 2010, our group developed a series of azobenzene-containing phosphines (**3**, Chart 1). They were expected to increase the cone angle of the ligand by *trans*-to-*cis* photoisomerization of the azobenzene fragments.[21] We envisioned that this morphological change would generate structures resembling those reported for bowl-shaped phosphines, which show enhanced catalytic activity compared to conventional triarylphosphine ligands in several catalytic reactions by imposing the coordination of only one ligand.[22] Preliminary results on their use as ligands in several catalytic processes (rhodium hydroformylation, palladium allylic alkylation, and rhodium hydrosilylation) showed only a marginal effect of the irradiation on the reaction outcome. A deeper analysis of the geometry of the ligands by molecular modeling showed that both *cis* and *trans* isomers of the azobenzene-phosphines would render ligands with similar cone angles, due to free rotation around the P–C bond of the ligand.

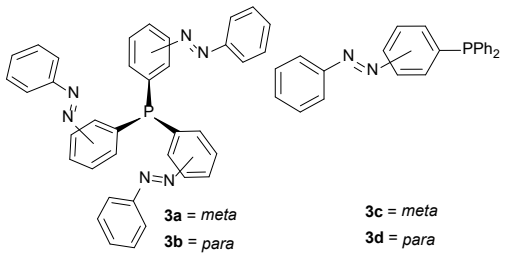

Chart 1. Azobenzene-phosphine ligands.

More recently, we reported the use of these photochromic ligands (among others) in the ruthenium-catalyzed hydrolysis of ammonia-borane (Figure 3).[23] The reaction profile, monitored

by measuring the hydrogen pressure generated, showed that the reaction rate could be externally regulated by alternating irradiation/dark periods. Although the change in activity was far from being a complete switch on/off of the catalytic properties, it represents a system for photo-controlled hydrogen generation from a chemical hydrogen storage material. The liberation of hydrogen was faster when the azobenzene fragments of the ligand were in the *Z* form. Additionally, similar results were obtained when *para*- (**3b**) or *meta*-substituted (**3a**) trisazobenzene-phosphines were used as ligands. These counterintuitive results indicated that, eventually, the increased activity observed upon *trans*-to-*cis* isomerization of the ligand most probably originated from electronic rather than from steric changes on the catalyst. This reasoning was in agreement with the electronic ligand effects previously observed when studying the reaction mechanism.[24] A series of azobenzene-containing bipyridines were also studied as ligands in this process. The effect of the *E*-*Z* isomerization on the reaction rate was less pronounced, and it also pointed to an electronic nature.[23]

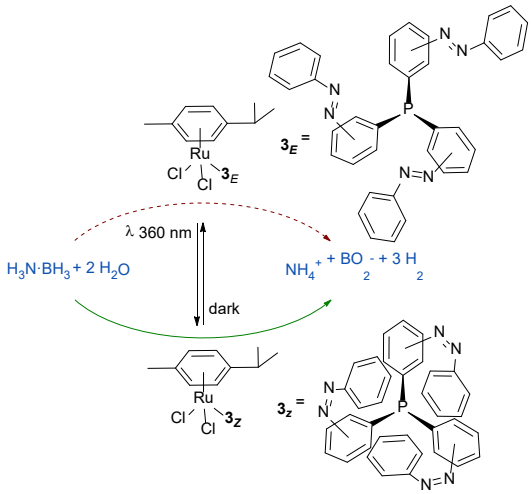

Figure 3. Photoswitchable hydrogen generation by ruthenium-catalysed hydrolysis of ammonia-borane. Green-continuous and red-dashed arrows represent faster and slower processes, respectively.

Eventually, light-induced electronic modifications on a coordinated ligand are a very effective strategy for the design of photoswitchable catalysts. In this context, N-heterocyclic carbene ligands (NHCs) are well-suited scaffolds to create a switchable catalyst, as the σ donating and π back-donating nature of the ligand strongly depends on the nature of the heterocyclic unit.[4b, 25] Based on this premise, the group of Yam developed a series of gold(I), silver(I), and palladium(II) complexes using NHC ligands annulated to a dithienylethene (DTE) photochromic actuator (**4**, **5** in Chart 2).[26] Within this design, and based on resonance contributions, photocyclization of the DTE fragment would reduce the electronic density on carbenoid atom of the annulated imidazole unit,[25b, 27] modifying the electronic properties of its organometallic complexes. Later on, the group of Bielawski confirmed this hypothesis experimentally by analyzing the CO stretching frequencies of the corresponding iridium(I) bis-carbonyl chloro complex (**6**).[28]

The calculated Tolman Electronic Parameters (TEP) revealed that whereas in the open form the value falls within the range expected for NHCs, the closed ligand TEP resembled that of phosphines.

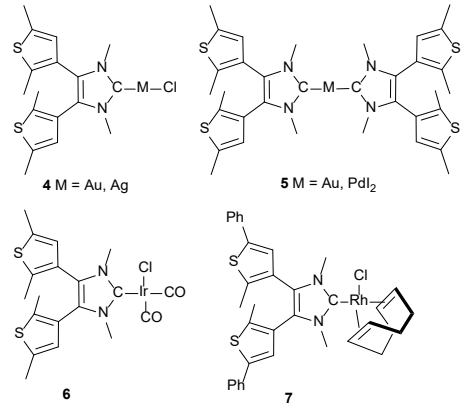

Chart 2. Au, Ag, Pd, Ir, and Rh DTE-NHC complexes developed by Yam and Sablowsky.[7d, 26, 28]

DTE-annulated NHCs were employed *per se* as photoswitchable organocatalysts.[7a, 29] Nearly simultaneously, they were integrated as ligands into organometallic catalysts. As a pioneering example, compound **7** was tested as a precatalyst in the hydroboration of alkenes and alkynes with pinacolborane (Figure 4).[7d] A 2.4 fold decrease in the reaction rate was observed upon pretreatment of the catalyst solution with UV-light when 1-octene was used as substrate. The ratio k_{vis}/k_{UV} was even more pronounced when styrene derivatives or *tert*-butylacetylene were used as substrates, attaining a value of 9.2 for styrene itself. The decrease in activity observed upon exposure of the catalyst to UV-light was attributed to a decrease in the electron-donating ability of the NHC-DTE ligand upon photocyclization. Thus, it reduced the facility of the catalyst to undergo reductive elimination, which (in agreement to previous studies on the process) is considered to be the rate-determining step (RDS). Additionally, the ability to switch between the two isomeric states of the catalyst was also utilized to alternatively change the rate of an ongoing hydroboration reaction by irradiation.

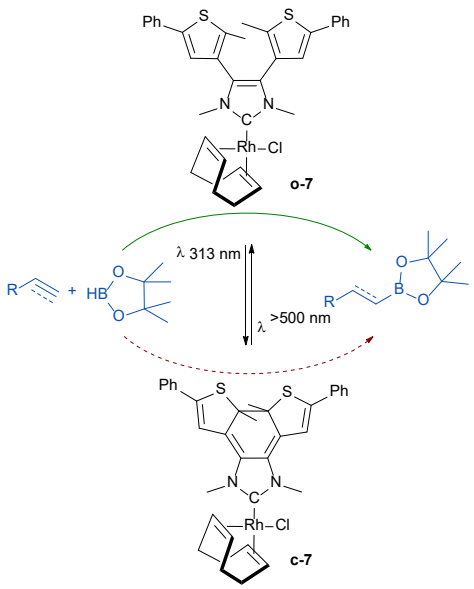

Figure 4. Photoswitchable hydroboration of unsaturated substrates catalyzed by rhodium DTE-NHC complex **7**. o and c prefixes stand for the open and closed forms of the DTE, respectively. Green-continuous and red-dashed arrows represent faster and slower processes, respectively.

The scope of this photoswitchable system was further extended to other catalytic processes. Substitution of the prototypical NHC ligand in the second-generation Hoveyda-Grubbs catalyst by a DTE-annulated NHC permitted Bielawski *et al*. to generate the first example of a photoswitchable olefin metathesis catalyst (**8** in Figure 5).[30]

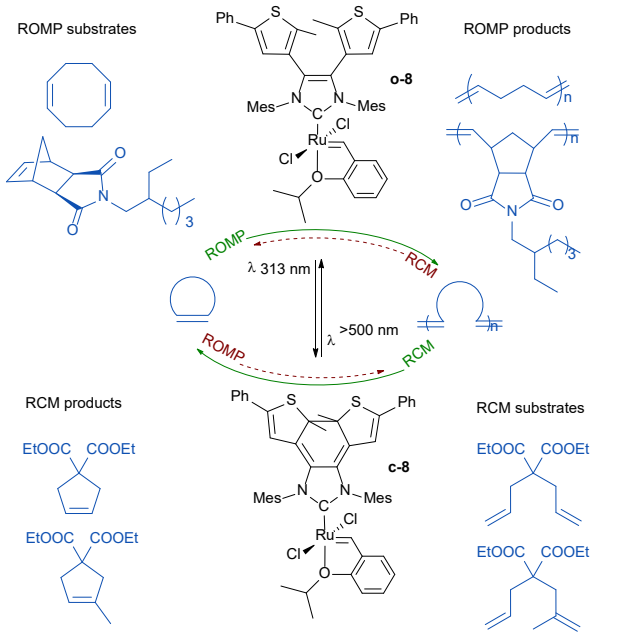

Figure 5. Photoswitchable olefin metathesis catalyzed by a ruthenium DTE-NHC complex **8**. o and c prefixes stand for the open and closed forms of the DTE, respectively. Green-continuous and red-dashed arrows represent faster and slower processes, respectively.

Complex **o-8** showed higher activity for the ROMP of 1,5-cis,cis-cyclooctadiene (COD) or norbornene (NBN) derivatives compared to the photo-stationary state (PSS) (containing 80% of **c-8**), $k_{o\text{-}8}/k_{PSS}$ = 1.5–1.8. The opposite trend was observed when **8** was applied to the ring-closing metathesis (RCM) of diethyl diallylmalonates ($k_{o\text{-}8}/k_{PSS}$ = 0.6–0.7). Helped by comprehensive density functional theory (DFT) calculations, the authors were able to rationalize the different relative activities in both processes. The lower activity of the open form of the catalyst in RCM was attributed to the higher donating ability of the carbene ligand in this isomeric form. It produces a stabilization of the Ru(IV) ruthenacycle intermediate, increasing the energy barrier for the subsequent retro-[2+2] cycloaddition, determined as the RDS of the reaction. In contrast, in the case of ROMP, a substrate dependence on the RDS of the process was observed. Whereas it was also the retro-[2+2] cycloaddition for the ROMP of COD, in the case of the NBN derivative, it was identified as the earlier [2+2] cycloaddition. In both cases, lower activation barriers were calculated for the open isomer of the catalyst. In the former, an electronic stabilization of [2+2]cycloaddition transition state (TS) when using the more electron-donating open form of the catalyst was claimed. However, higher steric repulsion between the mesityl substituents of the "planarized" closed ligand and the growing polymer chain in the corresponding TS were argued for the latter. In this example, as is often the case in organometallic catalysis, the eventual reaction rate is a fine balance between steric and electronic factors that stabilize/destabilize TSs and reaction intermediates. Therefore, the final effect is far from predictable and cannot be extrapolated to a broader range of substrates.

Although single off/on *in situ* catalytic experiments were reported, the system suffers from a relatively slow photoconversion and poor fatigue resistance under catalytic conditions.[5d]

There are also many examples of organometallic complexes in which a DTE core is an integral part of C–N[31] or N–N[32] chelating ligands, typically used in catalysis. With these ligands, a change in the electronic properties of the complex upon photocyclization could also be expected. Surprisingly, the only catalytic example that makes use of this strategy concerns the Cu-diphosphine system **9**.[33] A series of photoswitchable Cu(I) complexes were synthesized from a bimetallic chloro-bridged precursor containing two photochromic diphosphine ligands. The catalytic activity of an *in situ* generated Cu(I)-hydride containing the photochromic ligand was tested in the hydroboration of 4-fluorostyrene with pinacolborane (Figure 6). The catalyst showed slightly faster rates when the DTE-fragment was in the open form. Unfortunately, the reversibility of the process was not assessed with this derivative.

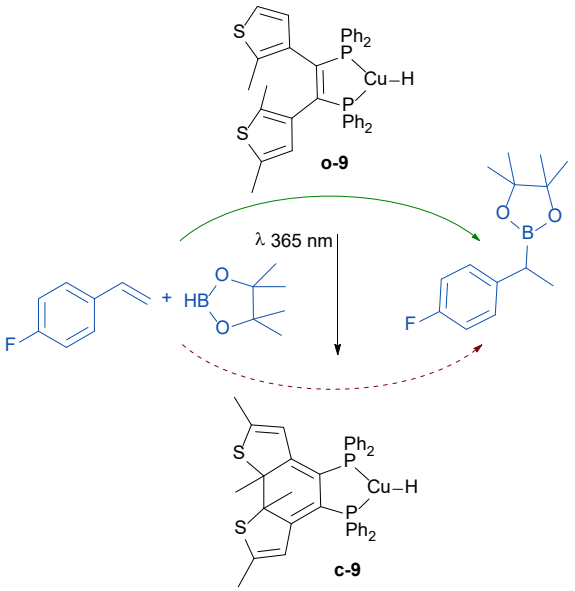

Figure 6. DTE-based diphosphine Cu(I) catalyst for hydroboration of 4-fluorostyrene with pinacolborane. The catalyst is described as a copper hydride formed by addition of KOtBu of a dimeric chloride-bridged precursor.[33] o and c prefixes stand for the open and closed forms of the DTE, respectively. Green-continuous and red-dashed arrows represent faster and slower processes, respectively.

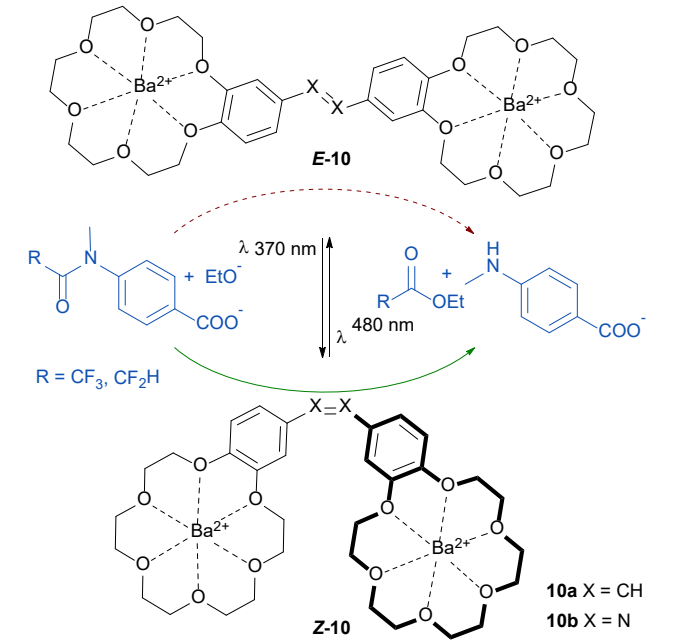

Figure 7. Bis-barium butterfly crown ether catalytic system. Green-continuous and red-dashed arrows represent faster and slower processes, respectively. For **10a** ***Z*-10** to ***E*-10** photoisomerization does not occur.

Bimetallic / Cooperative effects

An alternative design to construct catalysts with photoswitchable activity consists of using a photochromic ligand acting as a bridge between to catalytic metal ions. Either electronic or steric modifications on the ligand, upon irradiation, could control a cooperative effect between the two active centers. This strategy was exemplified in a seminal work by Cacciapaglia and Mandolini.[34] A bis(crown-ether) was studied as a ligand for the barium(II)-catalysed basic ethanolysis of esters and anilides (Figure 7). The first example, in which a stilbene was used as ligand scaffold (**10a**), already demonstrated the superior catalytic performance of the photogenerated *Z* form of the bimetallic complex when compared to the *E* isomer or a monometallic analog. Unfortunately, this preliminary system lacked reversibility. Replacement of the stilbene unit by an azobenzene rendered the so-called butterfly crown-ether bis-barium complex (**10b**),[35] which displayed photoreversibility and permitted the regulation of the catalytic activity by adjusting the excitation wavelength or the irradiation time in the course of a catalytic run. In this system, the barium centers act as distal anchoring groups for both the ethoxide anion and the carboxylate of the substrate. The improved activity observed when the catalyst is in the *Z* form was attributed to the concave shape of the ligand, bringing together the two Ba centers and, therefore, the two reactants (Figure 8).

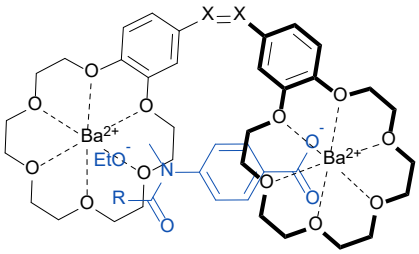

Figure 8. Synergistic mode of action of **Z-10**.

More recently, a related photoswitchable bimetallic catalyst was published by the group of Marinetti.[36] A bimetallic gold complex **11**, tethered by an azobenzene diphosphine, was used as a photoswitchable catalyst for the intramolecular hydroamination of an N-alkenyl urea (Figure 9). A fluorinated azobenzene backbone was used in order to increase the thermal stability of the *Z* isomer of the complex. Molecular structures, based on X-ray diffraction of crystalline samples of both isomers of a monometallic analog confirmed the stability of the *cis*-isomer, and allowed for a direct comparison of the structural parameters of the backbone in the *Z* an *E* forms.

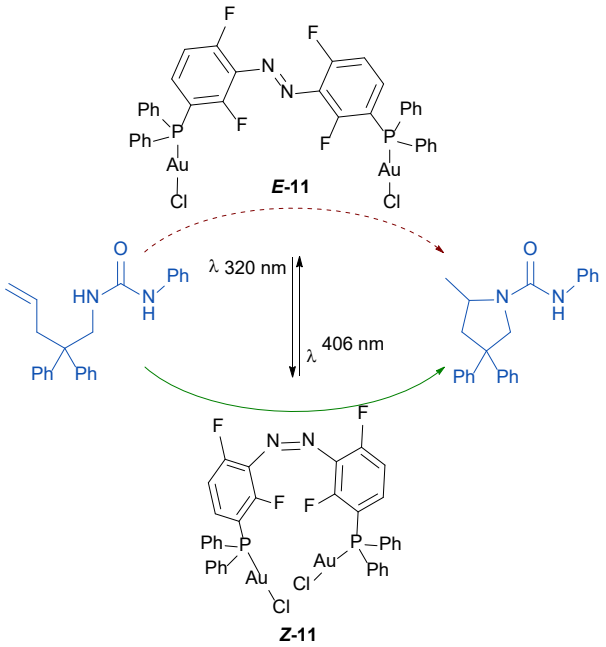

Figure 9. Photoswitchable bis-gold azobenzene-diphosphine catalytic system. Addition of 2eq. of silver salt ($AgSbF_6$) per mole of catalyst was required to initiate the process. Green-continuous and red-dashed arrows represent faster and slower processes, respectively.

When isolated samples of both isomers ***E*-11** and ***Z*-11** were used as catalyst, a slightly faster catalytic activity was observed for the *Z* compared to the *E* isomer. The latter showed a kinetic profile comparable to that of the monometallic analog, under identical conditions. Additionally, the catalytic activity could be modified during the reaction course by light-induced *trans*-to-*cis* isomerization of the azobenzene fragment in the ligand. These results pointed to a cooperative catalytic process being operative in the case of **Z-11**, and it was explained in terms of a bimetallic activation of both the olefin and urea functions of the substrate (Figure 10).

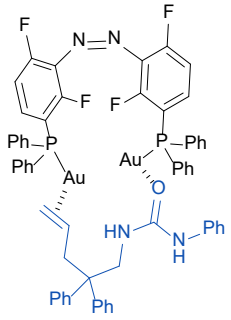

Figure 10. Synergistic mode of action of **Z-11**

The two systems described under this section are based on azobenzene ligand backbones that, acting as a hinge, control the distance between the two catalytic sites. Unfortunately, both showed considerable residual activity in the off state. Therefore, their behavior could be better described as a high/low switch of catalytic activity rather than as truly binary switches.

DTE could also be used as a photoactuators for the construction of photoswitchable binuclear catalysts. In this case, in addition to the clear structural modifications that photocyclization of a DTE-based bridging ligand could induce into a bimetallic system, open- and closed-DTE isomers also present rather different electronic properties, due to the extended π-electron conjugation of the closed form. This concept was first applied by the group of Branda.[37] They synthesized a DTE-diphosphine ligand and its corresponding bimetallic gold complex (**12a**, Figure 11). ^{31}P NMR analysis of a selenide derivative showed that ligand photocyclization increased the basicity of the phosphine in a similar manner to that caused by the substitution of a phenyl by an alkyl substituent on triphenylphosphine. The family of DTE-diphosphine ligands was extended further by Liu,[38] who also reported on the photochromic properties of their bimetallic gold(I) (**12b** and **12c**) and palladium(II) (**13**) derivatives (Figure 11).[39] These results anticipated the utility of such ligand to generate effective photoswitchable catalysts based on either steric or electronic modifications. Unfortunately, only the catalytic properties of the non-photochromic palladium dimer **13** were studied.

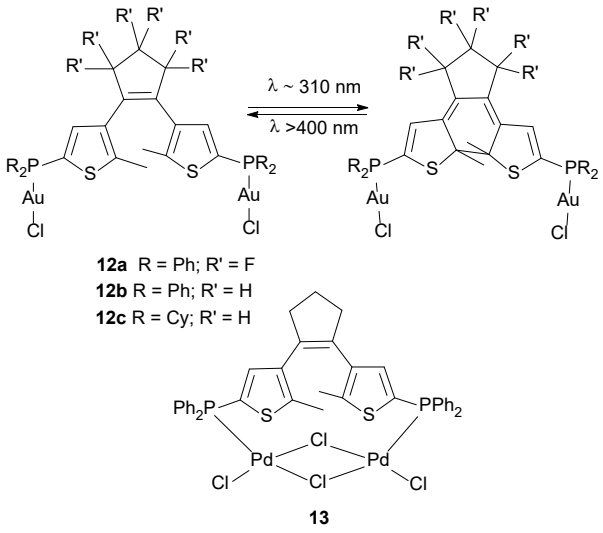

Figure 11. Bimetallic complexes based on DTE-diphosphine ligands.

Micellar catalysis.

Under the banner of green chemistry, many efforts have been devoted to the development of ligands with surfactant properties.[40] Such ligands are intended to enhance the catalytic activity in aqueous of biphasic media by increasing the solubility of the organic substrates in water through its inclusion in micellar catalytic nanostructures formed. Certainly, this is also a fascinating strategy for the construction of photoswitchable catalysis, provided that the surfactant properties of the ligand were photo-modulated. A photo-controlled formation of the micellar structures could *a priori* activate the catalytic process, and also facilitate the product recovery at the end of the reaction. In this vein, the group of Monflier developed a series of amphiphilic phosphine ligands based on an azobenzene photochromic unit (**14** Figure 12).[41] The role of the ligand was not only to tune the catalytic properties of the metal center, but also to solubilize in water both the metallic catalyst and the

hydrophobic substrate, triggering the catalytic process. The effect of UV-irradiation on the activity was studied on the Pd-catalyzed cleavage of allyl carbonates (Tsuji-Trost reaction). The results obtained with ligand **14b** showed a 2.5 fold enhancement of the catalytic activity upon UV irradiation, which was attributed to the formation of better-structured micellar aggregates when the ligand was in the *Z*-form. The difference was less evident with ligand **14a**.

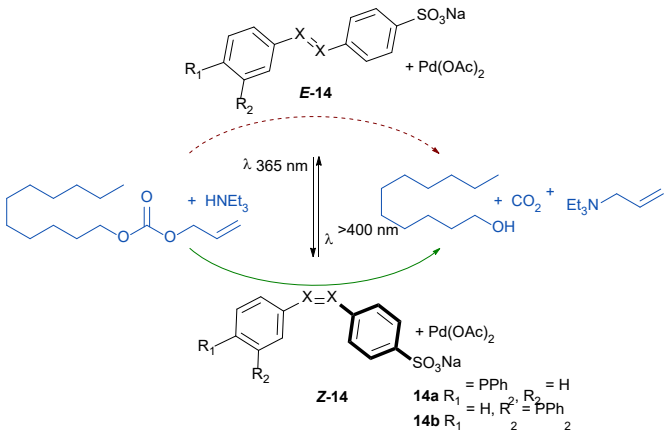

Figure 12. Photo-controlled micellar catalysis using ligand **13**. Green-continuous and red-dashed arrows represent faster and slower processes, respectively.

On a latter example, randomly modified β-cyclodextrins were added to the reaction mixture to improve the dynamics of the catalytic micellar system.[42] It is well-known that *trans*-azobenzene forms stable inclusion supramolecular structures with cyclodextrins, which were supposed to facilitate the aggregation dynamics in aqueous media. Unfortunately, the effect of irradiation on this supramolecular catalytic system was not reported.

3. Photoswitchable substrate selectivity.

Related to the previously described catalysis with photo-controlled activity, there is a specific situation in which a photoswitchable catalyst is able to display reverse on/off activities (or better high/low activities) towards specific substrates. Such a unique condition opens the possibility to construct systems with photo-controlled substrate affinity (Figure 13). Eventually, a catalyst operating in this mode could react preferentially with specific substrates from a reservoir containing a mixture of several of them in a spatio-temporal controlled manner.

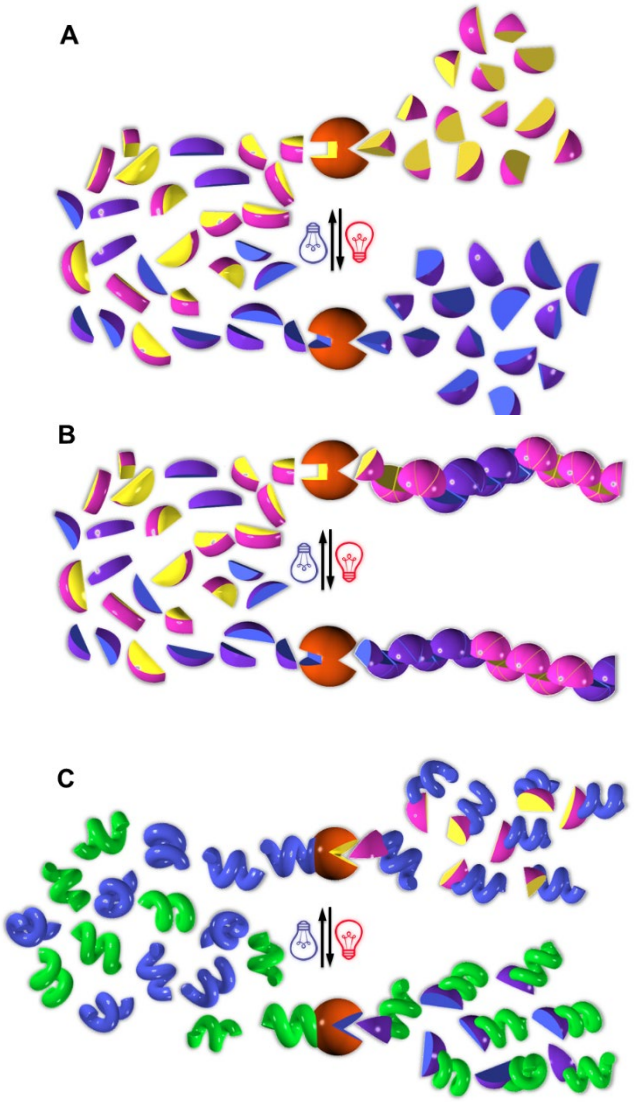

Figure 13. Catalyst with photoswitchable substrate selectivity. **A** Light-controlled product delivery from mixtures of substrates. **B** Synthesis of polymers with controlled composition and sequence. **C** Chiral resolution of racemic mixtures of substrates.

To the best of our knowledge, there is one recent example of a catalyst displaying such photo-controlled substrate discrimination. It is a salicylaldimine Zn(II) complex containing a tethered azobenzene photochromic unit (**15** in Figure 14).[43] The system, developed by Chen *et al.*, was studied as a catalyst for the ROP of cyclic esters.[43-44] The reactivity of the *E*- and *Z*-isomers of the catalyst towards several monomers was studied (Figure 14). The results showed that whereas a clear rate enhancement was observed for the *E*-isomer in the case of rac-lactide (LA) the relative reactivity was reversed for all the other monomers (up to 6 fold rate enhancement was observed for *Z*-isomer in the case of ε-caprolactone, CL). Additionally, the activity could be easily switched between the on/off states of the catalyst within a single run in homopolymerization processes. This privileged situation permitted the authors to carry out copolymerization experiments showing, for the first time, that it was possible to control the composition of the copolymer formed by means of irradiation. Although the origin of this light-induced substrate selectivity remains unclear,

authors proposed that it could be caused by electronic differences in the *cis*- and *trans*-isomeric complexes, discarding a steric origin of the discrimination.

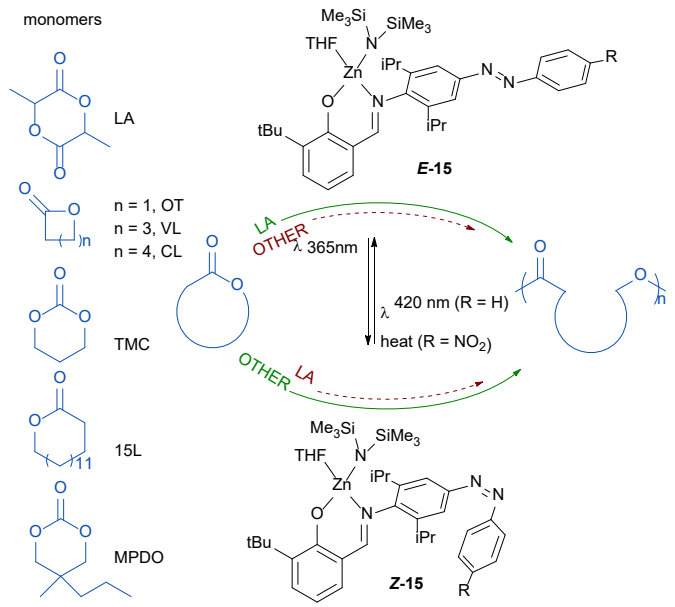

Figure 14. Zn(II) azobenzene-salicyladimide catalyst for photocrontrolled polymerization of cyclic esters. Green-continuous and red-dashed arrows represent fast and slow processes, respectively.

This only precedent will certainly inspire further developments, as the different possibilities that can be envisaged from this mode of action are fascinating. They range from already shown synthesis of polymers with controlled sequence and composition (Figure 13 B) to chiral resolution of racemic mixtures of substrates (Figure 13 C), or on-demand product delivery from mixtures of substrates (Figure 13 A), among others. Nevertheless, one must keep in mind that the strategy requires a precise selection of compatible substrates and catalysts, which is certainly not an easy task.

4. Photoswitchable stereoselectivity.

The capacity to deliver both enantiomers of a product is of paramount importance in pharmaceutical and bioorganic chemistry. When considering asymmetric catalysis for the synthesis of enantiopure compounds, the formation of energetically disparate diastereomeric substrate-catalysts transition states and/or reaction intermediates is the Holy Grail for success. In organometallic catalysis, with counted exceptions,[45] coordinated ligands are the source of chirality that drives the reaction in a stereoselective manner. Therefore, most of the effort in the area focusses on the development of highly sophisticated chiral ligands, often synthesized from the chiral pool.[46] One of the main drawbacks is that many natural synthons are available in only one absolute configuration. However, both enantiomeric ligands are required to produce opposite enantiomers of the same product. To circumvent this problem, in the last years, many efforts have been made to develop enantiodivergent catalysts. These systems can deliver both enantiomers of a product by changing the reaction conditions employed, or by introducing small structural modifications on a chiral catalyst.[7e, 47] A more sophisticated approach is the implementation of a dynamic control of the enantioselectivity of the catalyst by developing systems with stimuli-responding "chirality".[48] This strategy permits a given catalyst to produce enantiomeric products on-demand (Figure 15). In this sense, the development of photoswitchable ligands, able to generate pseudo enantiomeric catalysts through irradiation represents a milestone in the area.

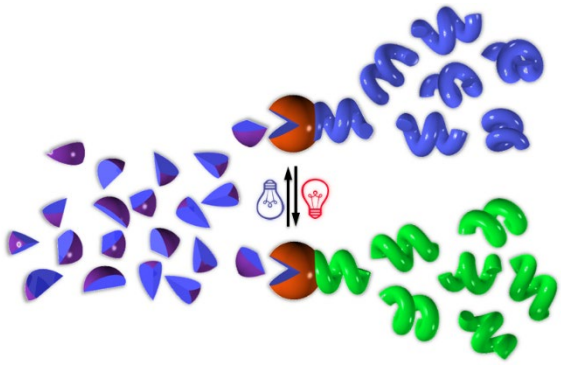

Figure 15. Catalyst with photoswitchable stereoselectivity.

Taking into account the "privileged" role that atropisomeric binaphthyl ligands play in asymmetric catalysis, not surprisingly one of the first attempts to develop a photoswitchable asymmetric catalyst was based on this motif. In 2002, the group of Kudo synthesized axially chiral phosphine ligands containing a proximal azobenzene fragment (**16**, Chart 3).[49] Compared to previously described azo-phosphines,[50] ligand **16** was designed to maximize the influence of the cis-trans photoisomerization on the reaction selectivity.

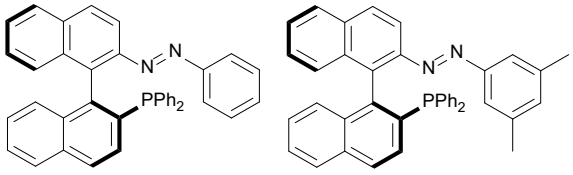

16a **16b**

Chart 3. Ligands **16** developed by Kudo.[49]

Unfortunately, when ligands **16** were tested in the Pd-catalyzed asymmetric allylic alkylation of *rac*-1,3-diphenyl-2-propenyl acetate using dimethylmalonate as nucleophile, no effect of the isomerization of the ligand on the enantioselectivity of the process was observed.

The first example of a catalyst able to show photo-controlled stereoselectivity was published in 2005 by Branda.[51] The authors' strategy was inspired by the leading position of chelating bisoxazoline ligands in asymmetric catalysis, that perfectly define a chiral environment at the catalytic site.[52] They synthesized a chiral bisoxazoline DTE ligand (Figure 16). It was anticipated that, in the open form, the ligand will act as a chiral chelate when reacting with Cu(I) salts. In contrast, UV-induced photocyclization will transform it into a ligand in which the two coordinating oxazolines will exist in a divergent disposition, therefore forming a monodentate complex.

The stereoselective cyclopropanation of styrene with ethyldiazoacetate was chosen as a test reaction. When the selectivity of the open form of the catalyst was compared to that obtained using a solution UV-irradiated to the PSS (23% **c-17**), a clear drop in enantioselectivity was observed. The difference was more evident when the reaction was carried out with an isolated sample of **c-17**. Additionally, the **o-17**-characteristic enantio and diastereoselectivities could be recovered by *in situ* irradiating the reaction mixture with visible light (λ > 434 nm). It is worth mentioning that, due to the stabilizing chelate effect, in the presence of copper, the reverse open-to-closed switch could only be accomplished when a coordinating co-solvent (CH_3CN) was used.

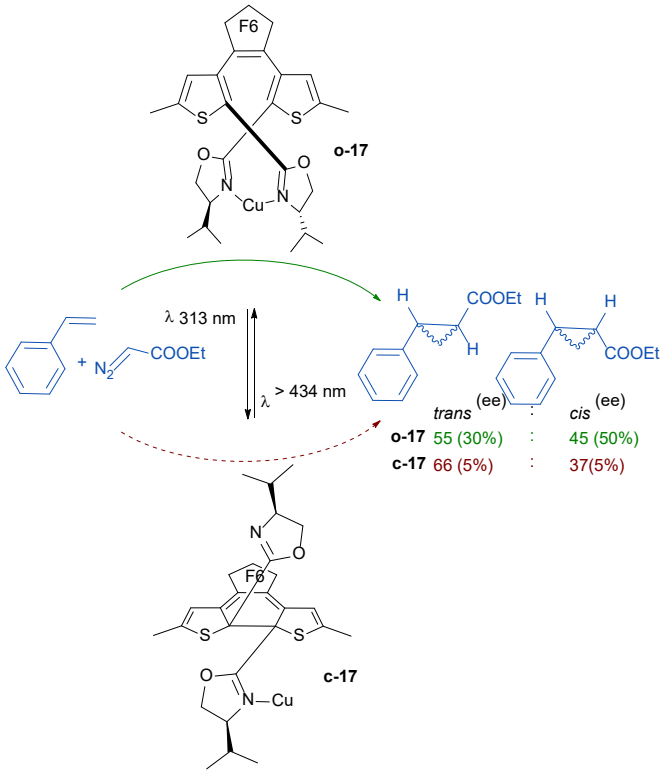

Figure 16. Cu(I) chiral bis(oxazoline)-DTE catalyst for the stereoselective cyclopropanation of styrene. o and c prefixes stand for the open and closed forms of the DTE, respectively. Green-continuous and red-dashed arrows represent processes displaying higher and lower stereoselectivities, respectively.

Although it was neglected in the case of catalyst **17**, one must keep in mind that DTE fragments are intrinsically chiral in the closed form, and also before photocyclization (provided that thiophene rings rotation was restricted), as stated in a previous publication of a related ligand.[53] Therefore, when using DTE derivatives containing additional stereogenic centers as ligands for asymmetric catalysis, the existence of diastereomeric mixtures of ligands is an important issue that should be addressed (or even exploited!).

In the aforementioned example, light induces the transformation of a chiral chelating ligand into a non-chelating one, being the change in the coordination mode of the ligand the origin of the different stereoinduction. In 2014, Craig *et al.* described a more subtle design. It addressed the modulation of the stereoselectivity of a catalytic system by light-induced distortion of the ligand geometry without altering the coordination mode nor the electronics of the coordinating fragment.[54] The ligand was a macrocyclic structure constructed by tethering a stiff stilbene (1,1'-bis-indanyliden) photochromic unit to a chiral atropisomeric bisphosphine ligand (**18** in Scheme 2). The actuator mechanism relied on the changes that *Z–E* photoisomerization of the stilbene unit embedded in the macrocyclic backbone of the ligand produces on the dihedral angle of the chelating diphosphine (ϕ). In such atropisomeric diphosphine ligands, it is well established that changes on ϕ have a profound influence on the regio- and stereoselectivity.[55] This relationship has been largely analyzed in several homogeneous catalytic processes using the **TunaPhos** family (Chart 4)[56]

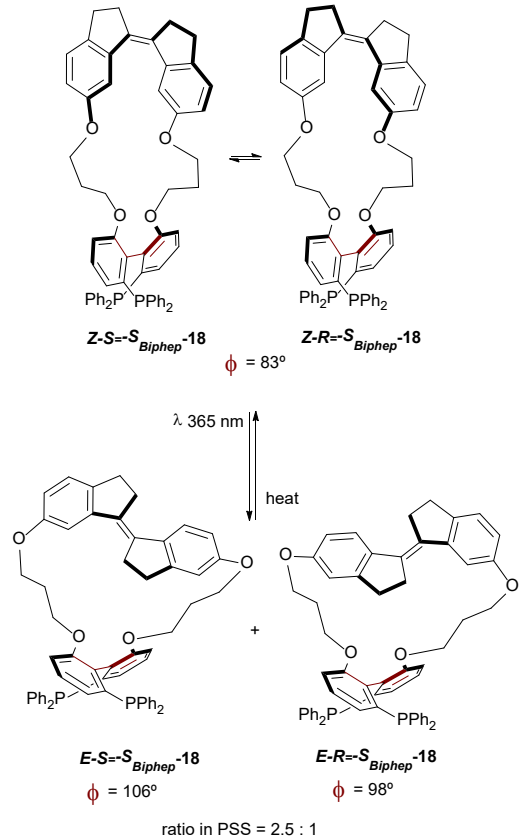

Scheme 2. Atropisomeric photoswitchable diphosphine ligands for photo-modulated asymmetric catalytic processes.

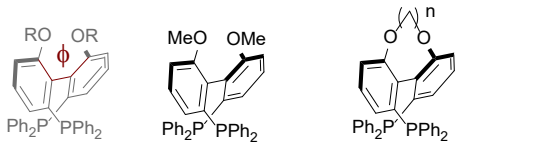

ϕ = 87° (97°) n = 1, ϕ = 60° n = 4, ϕ = 88°
n = 2, ϕ = 74° n = 5, ϕ = 94°
n = 3, ϕ = 77° n = 6, ϕ = 106°

Chart 4. Calculated dihedral angles for **MeOBiphep** and **Cn Tunaphos** ligands based on Molecular Mechanics (MM2).[56a] Value in parenthesis was recalculated by DFT for comparative purposes.[54]

The ligand was synthesized in the *Z*-S_{Biphep} form (***Z*-S$_{Biphep}$-18**) which exists as an unresolvable mixture of two diastereomeric conformers, due to the low barrier of isomerization across the alkene ($S_=/R_=$). The calculated ϕ (83°) in *Z*-S_{Biphep} is narrower than the one expected for the acyclic **MeOBiphep** (see Chart 4). Exposition to UV light triggers the *Z*-to-*E* isomerization of the stiff stilbene to form ***E*-18**, which consists of a pair of diastereoisomers (***E*-S$_=$-S$_{Biphep}$-18** and ***E*-R$_=$-S$_{Biphep}$-18**). The calculated ϕ of the former (106°) is larger than the one of **MeOBiphep** whereas the one of the latter shows a nearly undistorted biphep core (ϕ = 98°). It is worth mentioning that, despite the axial chirality generated in the stiff stilbene fragment upon *cis*-to-*trans* photoisomerization, the different ligand conformations are analyzed and described in terms of distortion of the natural ligand geometry rather than in terms of matching-mismatching of the chiral components of the ligand.

UV-irradiation of CH_2Cl_2 solutions of ***S*$_{Biphep}$-18** produced PSS composed by ***Z*-S$_{Biphep}$-18** / ***E*-S$_=$-S$_{Biphep}$-18** / ***E*-R$_=$-S$_{Biphep}$-18** = 68 / 23 / 9. Isolated samples of ***Z*-S$_{Biphep}$-18** and ***E*-S$_=$-S$_{Biphep}$-18** ligands, were individually tested as ligands in Pd-catalyzed asymmetric transformations (see Scheme 3). Despite the clear influence observed of the dihedral angle on the selectivity of the process on, in both cases, the fixed sense of the axial chirality of the OBiphep core dictates the major isomer produced. Additionally, a reaction run using an *in situ* generated PSS mixture of the corresponding Pd-catalysts showed the behavior expected for the mixture of compounds.

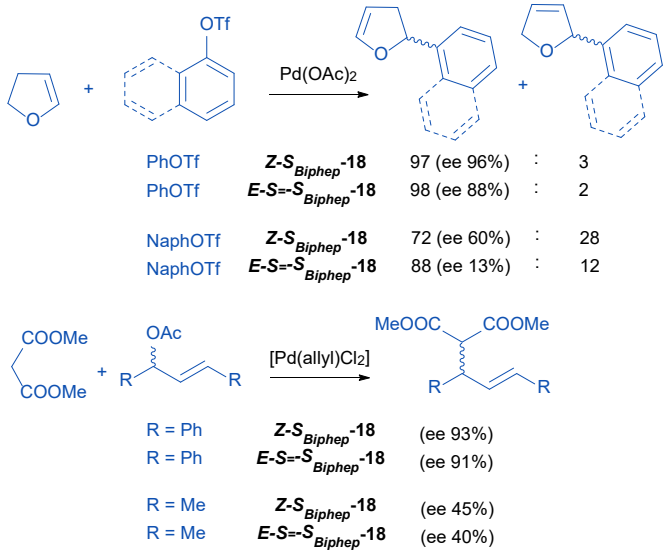

Scheme 3. Pd-catalyzed Heck arylation of 2,3-dinydrofurans (top) and Trost allylic alkylation of (+/-)-E-allylacetates using isolated ligands ***Z*-S$_{Biphep}$-18** and ***E*-S$_=$-S$_{Biphep}$-18**.

The relevance of this example, rather than on the absolute difference of the observed regio/enantioselectivities is the demonstration that including a photochromic actuator on the ligand backbone can be a powerful strategy to amplify/diminish the intrinsic ligand chirality.[57] Most probably, future catalysts based on this concept will appear, as there is plenty of room for improvement in terms of ligand design.

It is worth recalling that, even if the extent of the enantio-induction was modulated by the photochromic actuator, the handedness of the product was related to that of the biphep component, which remained unaltered due to its high atropisomerization barrier imposed by the *ortho* substituents. The next-generation catalysts would be those able to reverse the sense of the enantio-induction by means of irradiation. Such a system would permit obtaining each enantiomer of a chiral product on demand by using a single enantiomer of a catalyst. A prototype of such ambidextrous catalysts was reported in 2015 by Feringa's group.[58] They developed a chiral diphosphine ligand (**19**) based on Feringa's first-generation unidirectional rotary motor core. The *cis* form of the ligand exists as two pseudo-enantiomeric species **(*P*,*P*)-cis-(*R*,*R*)-19** and **(*M*,*M*-cis-(*R*,*R*)-19** (with reversal helicities), which can be interconverted by irradiation through ***trans*-19** (Scheme 4). As described before for the pristine stilbene-based rotor core, 360° unidirectional rotation occurs through a four-step cycle (two thermal helix inversion processes and two photochemical *cis-trans* isomerization steps).[59]

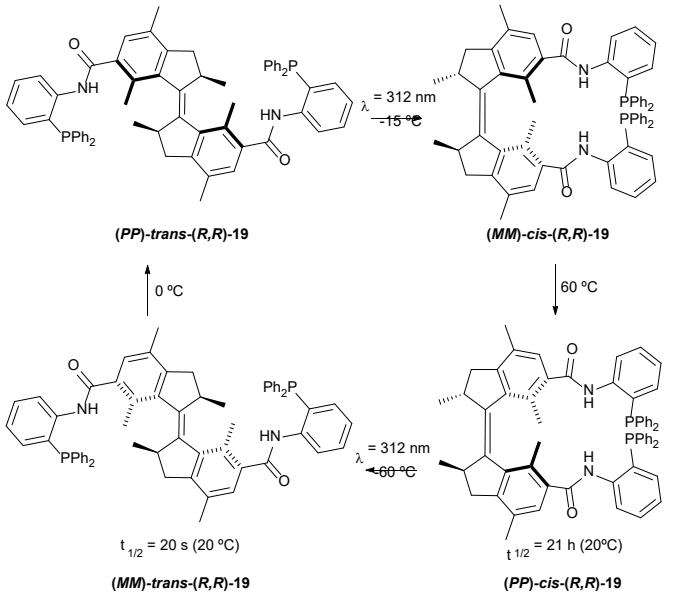

Scheme 4. Unidirectional rotary-cycle of ligand **19**.

The three most stable isomers of the ligand were independently tested in the Pd-catalyzed desymmetrization of *meso*-cyclopent-2-en-1,4-diol bis(carbamate) (Scheme 5). The results obtained showed that when the **(*P*,*P*)-trans-(*R*,*R*)-19** ligand was used a nearly racemic mixture of products was obtained. The lack of enantioinduction was explained due to the non-coordinating structure of the ligand, forced by the *trans* disposition of the stilbene core (as described before for DTE-based ligand in **17**). In contrast, when cisoid isomers were used the reaction proceeded with excellent stereocontrol, providing the corresponding oxazilidinones with enantiomeric ratios ~93/7. Remarkably, the light-controlled helicity of the ligand dictates the handedness of the product.

As described by the authors, this sophisticated system "affords switching between multiple stereochemical forms with distinct

ligand properties"[58] as it is possible to control not only the helical chirality of the coordinating *cis*-diphosphine but also to transform it at will into a non-coordinating ligand.

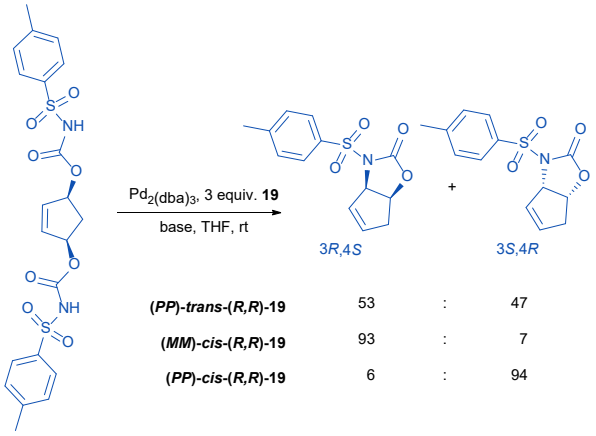

Scheme 5. Pd-catalyzed intramolecular cyclization of a *meso* bis(carbamate) using different isomers of ligand **19**.

Unfortunately, catalyst degradation under UV-irradiation hampered *in situ* switching of the catalyst. Supposing it was feasible, **(*P*,*P*)-cis-(*R*,*R*)-19** to **(*M*,*M*-cis-(*R*,*R*)-19** switch necessarily requires passing through unselective trasoid isomers, which would compromise the dynamic response of the catalyst.

In 2018, the same group developed a new system based on a second-generation unidirectional rotor containing a symmetrical fluorenyl group as one of the substituents of the alkene. This design avoids the existence of transoid structures, making possible a direct interconversion between two pseudo-enantiomeric forms of the ligand (A in Figure 17).[60] The highly sophisticated design is based on the synchronous motion observed between the light-controlled unidirectional rotation of an overcrowded alkene and that of a tied biaryl unit.[61]

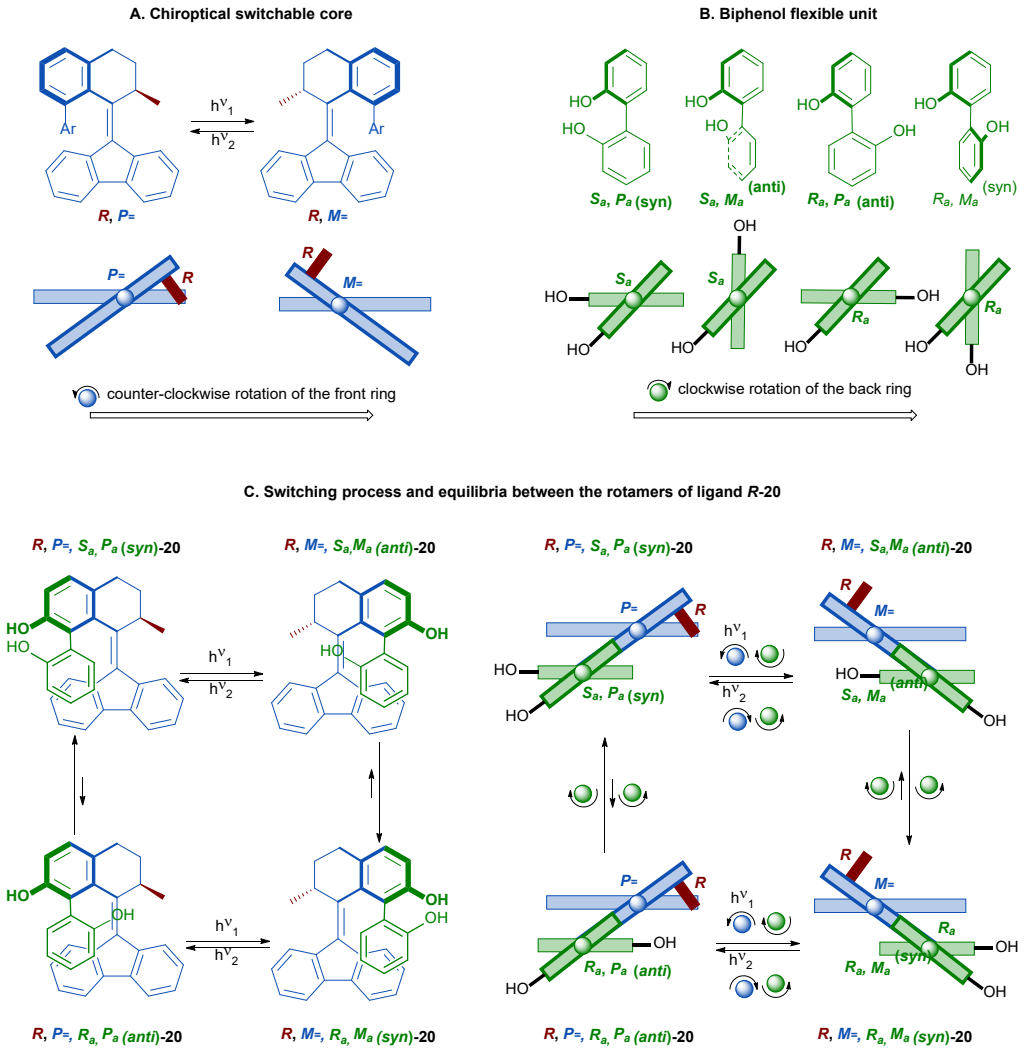

Figure 17. Conformational description of the possible isomers of the overcrowded alkene rotor (**A**), bisphenol unit (**B**) and *R*-**20** ligand (**C**). Top-down schematic representations have been included for clarity.

For steric reasons, from the four possible conformations of the biaryl (B in Figure 17) only those in which the nonnanulated aryl fragment is parallel to the fluorenyl component of the rotor are adopted (C in Figure 17). As a consequence of such tidal locking, the helicity of the biaryl (P_a/M_a) in any viable conformer of the ligand is necessarily identical to that of the central rotor ($P_=/M_=$). Taking into account these restrictions, and fixing the chirality of the stereogenic center (e.g. *R*), there are only four possible conformations of the ligand ***R*-20** (C in Figure 17): two biphenyl rotamers of the stable state (*R*, $P_=$) and two of the metastable state (*R*, *M*=). According to DFT calculations, the biphenyl atropisomerization equilibria are strongly displaced toward the *syn* conformations in both states (*R*, $P_=$, S_a, P_a and *R*, $M_=$, R_a, M_a, respectively), which is even more pronounced in presence of a bisphenol-chelating metal. These phenomena convert the system into the first photoswitchable ligand able to toggle directly between two pseudo-enantiomeric isomers.

The effectivity of the light-switchable chiral ligand ***R*-20** was tested in the enantioselective addition of organozinc to aromatic aldehydes. The results obtained showed that a clear reversal of the enantioselectivity of the product controlled by a light-induced switch of the ligand (Figure 18), being the first example of a truly ambidextral catalyst.

The working mechanism is based on an effective transfer of the light-controlled helical chirality of the overcrowded alkene to the axial chirality of and appended bisphenol unit. The control is driven by steric interactions, and eventually directed by the punctual chirality of the stereogenic center (Figure 17). These results can be considered a real milestone in the area. Further applications of this and related enantiodivergent photocontrolled systems will change the current panorama of asymmetric catalysis.

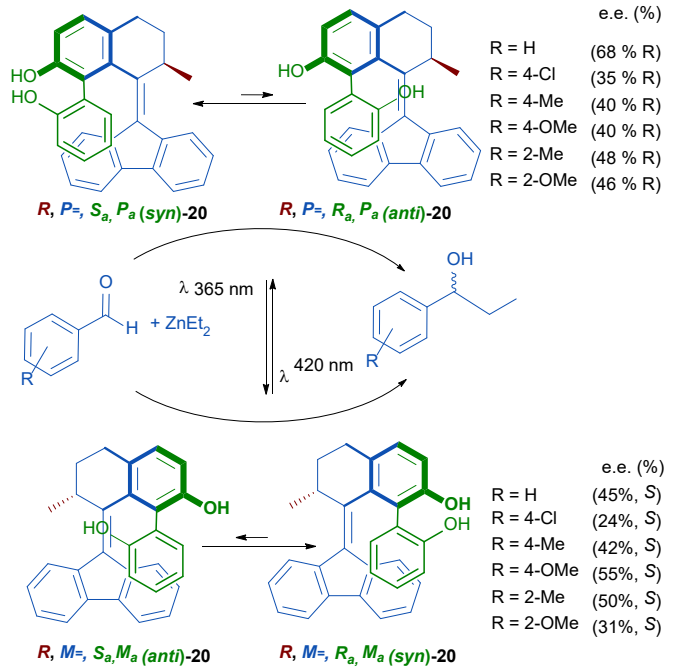

Figure 18. Light-controlled enantioselective addition of organozinc to aromatic aldehydes using ligand ***R*-20**.

5. Photoswitchable ligands with potential application in catalysis.

Several reviews on photochrome-coupled organometallics can be encountered in the literature, offering a comprehensive overview of the different chromophores and strategies used to implement photofunctionalities into organometallic complexes.[62] This information is a thesaurus for the development of future photofunctional organometallic catalysts. This section is a personal selection of some photochromic ligands biased by the perception that they could be easily transferred to catalysis. They pertain to the most representative families of ligands frequently used for the construction of homogeneous catalysts.

The most prolific family of actuators used for the construction of photoswitchable organometallics are the azobenzene derivatives. Several metal complexes of bipyridine,[23, 63] phenylpyridine,[64] or NHC ligands[65] containing appended azobenzene fragments have been published. Chart 5 shows representative examples. Light-induced morphological changes are evident. However, in most cases, ligand design needs further improvement to maximize the steric and/or electronic differences between both isomeric forms. Nevertheless, two azobenzene-based ligand types outstand due to their functional design: bipyridines **24**, and monodentate N-donors represented by **25**[66] and **26**[67] (Chart 6). These systems display a photocontrolled labilization/coordination to the metal center. In the former case (**24**), a reversible ligand exchange was observed between the corresponding Cu complexes and free bipyridine ligands present in solution.[63c, 63e]

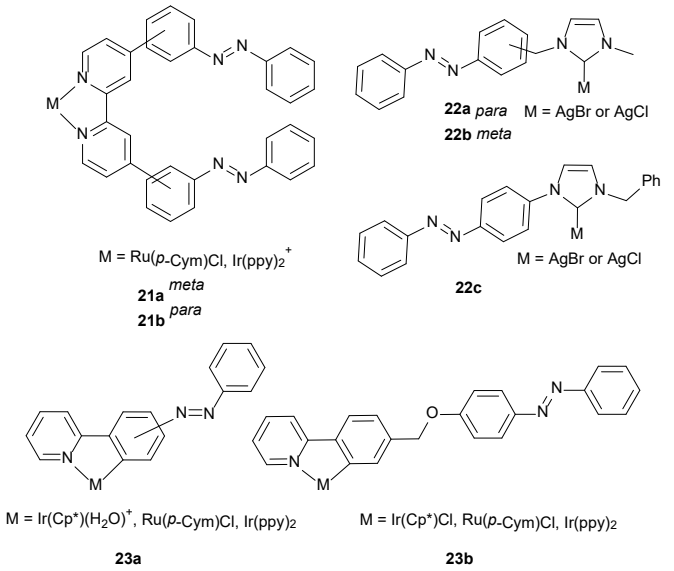

Chart 5. Representative examples of complexes containing azobenzene-appended bipyridine,[23, 63l] NHC,[65] and phenylpyridine[64] ligands.

The latter examples (**25** and **26**) were designed to display sterically-driven photomodulation of their axial coordination ability to Ni- or Zn-porphyrins, respectively. Despite the clear parallelism existing between these ligands and ligand **1**, no catalytic applications of such smart functional systems have been published yet.

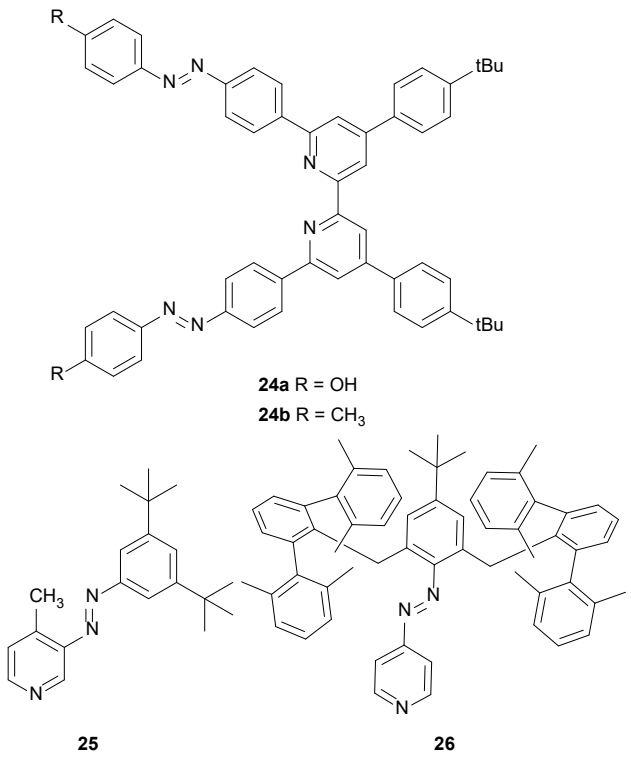

24a R = OH
24b R = CH_3

25 **26**

Chart 6. Photolabile azobenzene-based ligands.

DTE fragments have also been extensively used for the construction of photochromic ligands.[68] The evident light-induced shape modification occurring during DTE photocyclization, and the important electronic changes produced as a consequence of the 6π-intramolecular electrocyclization inspired many of the known photoswitchable catalysts (as seen in the former sections). However, some promising DTE-based ligands are still waiting for successful applications in catalysis.

In 2015, Wass and Scarso published a series of diphenylphosphine ligands directly bound to one thiophene ring of a DTE fragment (**27**, Chart 7).[69] By evaluating the magnitude of the P–Se NMR coupling constant of the corresponding phosphine selenide derivatives, they demonstrated that the electronic properties of the ligands could be photomodulated. Preliminary studies on the corresponding Pt(II) complexes showed that metal coordination inhibited DTE photoresponse. However, the similarity with the photoactive system **12** suggests that by selecting the appropriate metal it could turn into a photoswitchable catalyst.

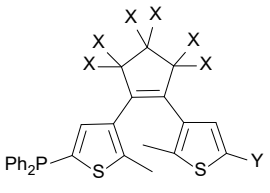

27a X = F, Y = Cl **27d** X = H, Y = Cl
27b X = F, Y = Ph **27e** X = H, Y = Ph
27c X = F, Y = C_6H_4OMe-*p* **27f** X = H, Y = C_6H_4OMe-*p*

Chart 7. DTE-based phosphine ligands with electronic phototunable properties.[69]

Interestingly, studies on ligands **27** showed that the influence of the electronic properties of the Y substituent on the phosphine basicity was larger on the closed-form compared to the open-form of the ligand, which confirms the electronic communication existing between the two thiophene fragments upon DTE photocyclization. As mentioned in section 2, this photo-controlled wirelike behavior depending on the open/close state of the DTE bridge could eventually encounter interesting applications in cooperative catalysis. Different families of DTE-bridged bimetallic complexes appeared in the literature containing organometallic structures that resemble those frequently used for catalytic purposes.[70] Some examples are shown in Chart 8. Among these examples, it is worth highlighting the DTE-bridged bis(copper) complex **29** in which not only a magnetic communication between the two metal centers was assessed, but also a photo-controlled copper coordination-ejection was observed in solution.

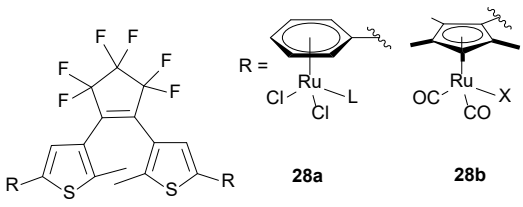

28a **28b**

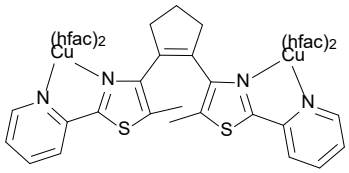

hfac = hexafluoroacetylacetoate

29

Chart 8. Representative examples of bimetallic complexes containing DTE-based bridging ligands.[70f, 70h]

As drawn from the examples described, DTE and azobenzene photochromes have been the actuators of choice for the construction of most of the functional catalysts described up to date. However, the use of other molecular switches cannot be discarded. In this sense, systems based on overcrowded alkenes molecular rotors seemed privileged for enantioselective processes. Therefore, other functional organometallic compounds based on overcrowded alkene molecular rotary motors are still waiting for catalytic applications.[71]

6. **Conclusions and outlook.**

The implementation of external control on homogeneous catalysts is a flourishing area of research. Many authors contributed to the state of the art tantalized by the belief that one day it will be possible to use cocktails of substrates and catalysts orthogonally controlled by light to produce specific products on demand. The examples provided herein evidence that it is not a chimera. However, there is still a long way to make it a reality. The roadmap to success requires a multidisciplinary approach, merging a profound understanding of homogeneous catalysis and of the photophysical properties of the photochromic actuators, through a rational ligand design.

Additionally, the optimization of the experimental conditions may not be trivial. Several factors confluence to make the current moment privileged to make real progress in the area. On the one hand, complex molecular machines incorporating photo-actuators have been developed in the last decades. The implementation of such smart chemical systems into known functional catalysts represents a win to win strategy, as demonstrated by the successful examples coming from Feringa's group. On the other hand, the astonishing advance that photoredox catalysis is experiencing triggered a fast evolution of the experimental setup needed to handle catalytic reactions under specific irradiation conditions, making photoreactors (home-made and also commercially available) accessible to most of the research laboratories. Last but not least, homogeneous catalysis is a mature area of research. Nowadays, many catalytic processes are well understood, including the ligand properties that most affect the catalytic outcome.

Concerning ligand design, there is plenty of room for improvement as concluded from the examples described herein. Surprisingly, the most effective systems developed up to now involve the rather challenging enantioselective processes whereas the photo-control of "more simple" aspects of the catalytic event (i.e. chemo- or regioselectivity, solvent affinity, heterogenization) remains virtually unexplored.

Polymerization reactions stand out as one of most successfully photocontrolled processes showing that it is possible to control both, the catalyst activity and the substrate sensitivity. The combination of these actuators in a single process (or including other functionalities such as the remote control on the stereochemical insertion of monomers) using orthogonal stimuli would offer new venues in the field of materials science.

To sum up, it is clear that we are enjoying the early days of a fascinating development. There are no rules established yet. However, the basic tools provided, which is the ideal scenario for creative scientists to flourish.

Conflicts of interest

There are no conflicts to declare.

Acknowledgements

Funding from Ikerbasque, Basque Government (IT1180-19) and Ministry of Science, Innovation and Universities (RED2018-102471-T) is acknowledged. A. I. Aranburu Leiva is kindly acknowledged for proofreading the manuscript.

Notes and references

‡ Strictly speaking, an organometallic compound should contain a bond between a C atom and the metal center, but in this review, mono or bimetallic compounds constructed with ligands based on N, P, or O donors will be also included, as it is always the case when referring to organometallic catalysis.[1, 72]

1. P. W. N. M. van Leeuwen, *Homogeneous Catalysis, Understanding the Art*, Kluver AP, Dordrecht, 2004.
2. R. Göstl, A. Senf and S. Hecht, *Chem. Soc. Rev.*, 2014, **43**, 1982-1996.
3. Z. Freixa and P. W. N. M. van Leeuwen, *Dalton Trans.*, 2003, 1890-1901.
4. (a) R. H. Crabtree, *New J. Chem.*, 2011, **35**, 18-23; (b) E. Peris, *Chem. Rev.*, 2018, **118**, 9988-10031; (c) V. Blanco, D. A. Leigh and V. Marcos, *Chem. Soc. Rev.*, 2015, **44**, 5341-5370; (d) T. Imahori, in *Designed Molecular Space in Material Science and Catalysis*, ed. S. Shirakawa, Springer Singapore, Singapore, 2018, pp. 227-245; (e) J. Choudhury, *Tetrahedron Lett.*, 2018, **59**, 487-495; (f) N. Kumagai and M. Shibasaki, *Catal. Sci. Technol.*, 2013, **3**, 41-57.
5. (a) H. Lai, J. Zhang, F. Xing and P. Xiao, *Chem. Soc. Rev.*, 2020, **49**, 1867-1886; (b) N. Corrigan and C. Boyer, *ACS Macro Letters*, 2019, **8**, 812-818; (c) F. A. Leibfarth, K. M. Mattson, B. P. Fors, H. A. Collins and C. J. Hawker, *Angew. Chem. Int. Ed.*, 2013, **52**, 199-210; (d) S. P. Ihrig, F. Eisenreich and S. Hecht, *Chem. Commun.*, 2019, **55**, 4290-4298.
6. B. M. Neilson and C. W. Bielawski, *ACS Catal.*, 2013, **3**, 1874-1885.
7. (a) B. M. Neilson and C. W. Bielawski, *J. Am. Chem. Soc.*, 2012, **134**, 12693-12699; (b) Z. Yu and S. Hecht, *Chem. Commun.*, 2016, **52**, 6639-6653; (c) S. M. Guillaume, E. Kirillov, Y. Sarazin and J.-F. Carpentier, *Chem. Eur. J*, 2015, **21**, 7988-8003; (d) B. M. Neilson and C. W. Bielawski, *Organometallics*, 2013, **32**, 3121-3128; (e) G. Romanazzi, L. Degennaro, P. Mastrorilli and R. Luisi, *ACS Catal.*, 2017, **7**, 4100-4114; (f) A. J. Teator and C. W. Bielawski, *J. Polym. Sci. Part A: Polym. Chem.*, 2017, **55**, 2949-2960; (g) R. S. Stoll and S. Hecht, *Angew. Chem. Int. Ed.*, 2010, **49**, 5054-5075; (h) R. Dorel and B. L. Feringa, *Chem. Commun.*, 2019, **55**, 6477-6486; (i) C. E. Diesendruck, O. Iliashevsky, A. Ben-Asuly, I. Goldberg and N. G. Lemcoff, *Macromol. Symp.*, 2010, **293**, 33-38.
8. (a) K. M. Waltz and J. F. Hartwig, *Science*, 1997, **277**, 211-213; (b) Z.-F. Zhang and M.-D. Su, *RSC Adv.*, 2018, **8**, 10987-10998.
9. D. Burget, T. Mayer, G. Mignani and J. P. Fouassier, *J. Photochem. Photobiol. A*, 1996, **97**, 163-170.
10. D. Wang, K. Wurst, W. Knolle, U. Decker, L. Prager, S. Naumov and M. R. Buchmeiser, *Angew. Chem. Int. Ed.*, 2008, **47**, 3267-3270.
11. L. Delaude, A. Demonceau and A. F. Noels, *Chem. Commun.*, 2001, 986-987.
12. B. K. Keitz and R. H. Grubbs, *J. Am. Chem. Soc.*, 2009, **131**, 2038-2039.
13. (a) A. Hafner, A. Mühlebach and P. A. van der Schaaf, *Angew. Chem. Int. Ed.*, 1997, **36**, 2121-2124; (b) G. Bhukta, R. Manivannan and G. Sundararajan, *J. Organomet. Chem.*, 2000, **601**, 16-21; (c) E. Levin, S. Mavila, O. Eivgi, E. Tzur and N. G. Lemcoff, *Angew. Chem. Int. Ed.*, 2015, **54**, 12384-12388; (d) T. Karlen, A. Ludi, A. Mühlebach, P. Bernhard and C. Pharisa, *J. Polym. Sci. Pol. Chem.*, 1995, **33**, 1665-1674; (e) D. Wang, J. Unold, M. Bubrin, I. Elser, W. Frey, W. Kaim, G. Xu and M. R. Buchmeiser, *Eur. J. Inorg. Chem.*, 2013, **2013**, 5462-5468; (f) Y. Vidavsky and N. G. Lemcoff, *Beilstein J. Org. Chem.*, 2010, **6**, 1106-1119; (g) W. Joo, C. H. Chen, J. P. Moerdyk, R. P. Deschner, C. W. Bielawski and C. G. Willson, *J. Polym. Sci. Pol. Chem.*, 2019, **57**, 1791-

1795; (h) S. Naumann and M. R. Buchmeiser, *Macromol. Rapid Commun.*, 2014, **35**, 682-701; (i) D. Wang, K. Wurst and M. R. Buchmeiser, *Chem. Eur. J*, 2010, **16**, 12928-12934; (j) P. A. van der Schaaf, A. Hafner and A. Mühlebach, *Angew. Chem. Int. Ed.*, 1996, **35**, 1845-1847.

14. (a) R. N. Perutz and B. Procacci, *Chem. Rev.*, 2016, **116**, 8506-8544; (b) M. R. Buchner, B. Bechlars and K. Ruhland, *J. Organomet. Chem.*, 2013, **744**, 60-67.
15. (a) J. Pinaud, T. K. H. Trinh, D. Sauvanier, E. Placet, S. Songsee, P. Lacroix-Desmazes, J.-M. Becht, B. Tarablsi, J. Lalevée, L. Pichavant, V. Héroguez and A. Chemtob, *Chem. Eur. J.*, 2018, **24**, 337-341; (b) L. Pichavant, P. Lacroix-Desmazes, A. Chemtob, J. Pinaud and V. Héroguez, *Polymer*, 2020, **190**, 122200; (c) T. K. H. Trinh, G. Schrodj, S. Rigolet, J. Pinaud, P. Lacroix-Desmazes, L. Pichavant, V. Héroguez and A. Chemtob, *RSC Adv.*, 2019, **9**, 27789-27799; (d) L. Pichavant, P. Lacroix-Desmazes, A. Chemtob, J. Pinaud and V. Héroguez, *Polym. Chem.*, 2018, **9**, 5491-5498.
16. H. Sugimoto, T. Kimura and S. Inoue, *J. Am. Chem. Soc.*, 1999, **121**, 2325-2326.
17. T. Aida and S. Inoue, *J. Am. Chem. Soc*, 1983, **105**, 1304-1309.
18. Y. Iseki and S. Inoue, *J. Chem. Soc., Chem. Commun.*, 1994, 2577-2578.
19. C. Deo, N. Bogliotti, P. Retailleau and J. Xie, *Organometallics*, 2016, **35**, 2694-2700.
20. C. Deo, N. Bogliotti, R. Métivier, P. Retailleau and J. Xie, *Organometallics*, 2015, ASAP Dec. 2015.
21. M. D. Segarra-Maset, P. W. N. M. van Leeuwen and Z. Freixa, *Eur. J. Inorg. Chem.*, 2010, 2075-2078.
22. (a) O. Niyomura, M. Tokunaga, Y. Obora, T. Iwasawa and Y. Tsuji, *Angew. Chem. Int. Ed.*, 2003, **42**, 1287-1289; (b) A. Ochida and M. Sawamura, *Chem. Asian J.*, 2007, **2**, 609-618; (c) Y. Ohzu, K. Goto and T. Kawashima, *Angew. Chem. Int. Ed.*, 2003, **42**, 5714-5717; (d) Y. Ohzu, K. Goto, H. Sato and T. Kawashima, *J. Organomet. Chem*, 2005, **690**, 4175-4183; (e) T. Iwai and M. Sawamura, *Bull. Chem. Soc. Jpn.*, 2014, **87**, 1147-1160.
23. A. Telleria, P. W. N. M. Van Leeuwen and Z. Freixa, *Dalton Trans.*, 2017, **46**, 3569-3578.
24. A. Telleria, C. Vicent, V. San Nacianceno, M. A. Garralda and Z. Freixa, *ACS Catal.*, 2017, **7**, 8394-8405.
25. (a) S. Fantasia, J. L. Petersen, H. Jacobsen, L. Cavallo and S. P. Nolan, *Organometallics*, 2007, **26**, 5880-5889; (b) Y. Ryu, G. Ahumada and C. W. Bielawski, *Chem. Commun.*, 2019, **55**, 4451-4466.
26. V. W.-W. Yam, J. K.-W. Lee, C.-C. Ko and N. Zhu, *J. Am. Chem. Soc.*, 2009, **131**, 912-913.
27. (a) T. Nakashima, M. Goto, S. Kawai and T. Kawai, *J. Am. Chem. Soc*, 2008, **130**, 14570-14575; (b) G. Duan, N. Zhu and V. W.-W. Yam, *Chem. Eur. J*, 2010, **16**, 13199-13209.
28. B. M. Neilson, V. M. Lynch and C. W. Bielawski, *Angew. Chem. Int. Ed.*, 2011, **50**, 10322-10326.
29. B. M. Neilson and C. W. Bielawski, *Chem. Commun.*, 2013, **49**, 5453-5455.
30. A. J. Teator, H. Shao, G. Lu, P. Liu and C. W. Bielawski, *Organometallics*, 2017, **36**, 490-497.
31. (a) G. Duan, W.-T. Wong and V. W.-W. Yam, *New J. Chem.*, 2011, **35**, 2267-2278; (b) J. C.-H. Chan, W. H. Lam, H.-L. Wong, N. Zhu, W.-T. Wong and V. W.-W. Yam, *J. Am. Chem. Soc.*, 2011, **133**, 12690-12705.
32. (a) V. W.-W. Yam, C.-C. Ko and N. Zhu, *J. Am. Chem. Soc.*, 2004, **126**, 12734-12735; (b) C.-C. Ko, W.-M. Kwok, V. W.-W. Yam and D. L. Phillips, *Chem. Eur. J*, 2006, **12**, 5840-5848; (c) T.-W. Ngan, C.-C. Ko, N. Zhu and V. W.-W. Yam, *Inorg. Chem.*, 2007, **46**, 1144-1152; (d) J. K.-W. Lee, C.-C. Ko, K. M.-C. Wong, N. Zhu and V. W.-W. Yam, *Organometallics*, 2007, **26**, 12-15; (e) P. H.-M. Lee, C.-C. Ko, N. Zhu and V. W.-W. Yam, *J. Am. Chem. Soc*, 2007, **129**, 6058-6059; (f) H.-L. Wong, N. Zhu and V. W.-W. Yam, *J. Organomet. Chem*, 2014, **751**, 430-437.
33. Z. Xu, Y. Cao, B. O. Patrick and M. O. Wolf, *Chem. Eur. J.*, 2018, **24**, 10315-10319.
34. R. Cacciapaglia, S. Di Stefano and L. Mandolini, *J. Org. Chem.*, 2002, **67**, 521-525.
35. R. Cacciapaglia, S. Di Stefano and L. Mandolini, *J. Am. Chem. Soc*, 2003, **125**, 2224-2227.
36. T. Arif, C. Cazorla, N. Bogliotti, N. Saleh, F. Blanchard, V. Gandon, R. Métivier, J. Xie, A. Voituriez and A. Marinetti, *Cat. Sci. Technol.*, 2018, **8**, 710-715.
37. D. Sud, R. McDonald and N. R. Branda, *Inorg. Chem.*, 2005, **44**, 5960-5962.
38. J. Yin, Y. Lin, X. Cao, G.-A. Yu, H. Tu and S. H. Liu, *Dyes Pigments*, 2009, **81**, 152-155.
39. J. Liang, J. Yin, Z. Li, C. Zhang, D. Wu and S. H. Liu, *Dyes Pigm.*, 2011, **91**, 364-369.
40. T. Dwars, E. Paetzold and G. Oehme, *Angew. Chem. Int. Ed.*, 2005, **44**, 7174-7199.
41. H. Bricout, E. Banaszak, C. Len, F. Hapiota and E. Monflier, *Chem. Commun.*, 2010, **46**, 7813-7815.
42. (a) H. Bricout, E. Léonard, C. Len, D. Landy, F. Hapiot and E. Monflier, *Beilstein J. Org. Chem.*, 2012, **8**, 1479-1484; (b) M. Ferreira, H. Bricout, N. Azaroual, D. Landy, S. Tilloy, F. Hapiot and E. Monflier, *Adv. Synth. Catal.*, 2012, **354**, 1337-1346; (c) F. Hapiot and E. Monflier, *Catalysis*, 2017, **7**, 173; (d) E. Léonard, F. Mangin, C. Villette, M. Billamboza and C. Len, *Catal. Sci. Technol.*, 2016, **6**, 379-398.
43. M. Li, P. Zhang and C. Chen, *Macromolecules*, 2019, DOI: 10.1021/acs.macromol.9b00984.
44. J. Sun, *Chem. Res. Chinese Universities*, 2019, **116**, 116.
45. (a) L. Zhang and E. Meggers, *Chem. Asian J.*, 2017, **12**, 2335-2342; (b) Y. Zheng, Y. Tan, K. Harms, M. Marsch, R. Riedel, L. Zhang and E. Meggers, *J. Am. Chem. Soc.*, 2017, **139**, 4322-4325; (c) X. Shen, H. Huo, C. Wang, B. Zhang, K. Harms and E. Meggers, *Chem. Eur. J*, 2015, **21**, 9492-9726.
46. H. U. Blaser, *Chem. Rev.*, 1992, **92**, 935-952.
47. (a) T. Tanaka and M. Hayashi, *Synthesis*, 2008, **2008**, 3361-3376; (b) J. Escorihuela, M. I. Burguete and S. V. Luis, *Chem. Soc. Rev.*, 2013, **42**, 5595-5617; (c) J. Dai, Z. Wang, Y. Deng, L. Zhu, F. Peng, Y. Lan and Z. Shao, *Nat. Commun.*, 2019, **10**, 5182; (d) I. P. Beletskaya, C. Nájera and M. Yus, *Chem. Rev.*, 2018, **118**, 5080-5200; (e) W. Cao, X. Feng and X. Liu, *Org. Biomol. Chem.*, 2019, **17**, 6538-6550.
48. M. Vlatković, L. Bernardi, E. Otten and B. L. Feringa, *Chem. Commun.*, 2014, **50**, 7773-7775.
49. N. Kawamura, R. Kiyotake and K. Kudo, *Chirality*, 2002, **14**, 724-726.
50. M. J. Alder, W. I. Cross, K. R. Flower and R. G. Pritchard, *J. Chem. Soc., Dalton Trans.*, 1999, 2563-2573.
51. D. Sud, T. B. Norsten and N. R. Branda, *Angew. Chem. Int. Ed.*, 2005, **44**, 2019-2021.

52. (a) H. A. McManus and P. J. Guiry, *Chem. Rev.*, 2004, **104**, 4151-4202; (b) A. V. Bedekar, E. B. Koroleva and P. G. Andersson, *J. Org. Chem.*, 1997, **62**, 2518-2526.
53. E. Murguly, T. B. Norsten and N. R. Branda, *Angew. Chem. Int. Ed.*, 2001, **40**, 1752-1755.
54. Z. S. Kean, S. Akbulatov, Y. Tian, R. A. Widenhoefer, R. Boulatov and S. L. Craig, *Angew. Chem. Int. Ed.*, 2014, **126**, 14736-14739.
55. W. Tang and X. Zhang, *Chem. Rev.*, 2003, **103**, 3029-3070.
56. (a) Z. Zhang, H. Qian, J. Longmire and X. Zhang, *J. Org. Chem.*, 2000, **65**, 6223-6226; (b) S. Wu, W. Wang, W. Tang, M. Lin and X. Zhang, *Org. Lett.*, 2002, **4**, 4495-4497; (c) M. Raghunath and X. Zhang, *Tetrahedron Lett.*, 2005, **46**, 8213-8216.
57. N. Zhu, X. Li, Y. Wang and X. Ma, *Dyes Pigments*, 2016, **125**, 259-265.
58. D. Zhao, T. M. Neubauer and B. L. Feringa, *Nature Commun.*, 2015, **6**, 6652.
59. (a) F. Liu and K. Morokuma, *J. Am. Chem. Soc.*, 2012, **134**, 4864-4876; (b) M. M. Pollard, A. Meetsma and B. L. Feringa, *Org. Biomol. Chem.*, 2008, **6**, 507-512.
60. S. F. Pizzolato, P. Štacko, J. C. M. Kistemaker, T. van Leeuwen, E. Otten and B. L. Feringa, *J. Am. Chem. Soc*, 2018, **140**, 17278-17289.
61. P. Štacko, J. C. M. Kistemaker, T. van Leeuwen, M.-C. Chang, E. Otten and B. L. Feringa, *Science*, 2017, **356**, 964.
62. (a) S. Kume and H. Nishihara, *Dalton Trans.*, 2008, **25**, 3260-3364; (b) C.-C. Ko and V. W.-W. Yam, *Acc. Chem. Res.*, 2018, **51**, 149-159; (c) A. S. Abd-el-aziz and E. A. Strohm, in *Molecular design and applications of photofunctional polymers and materials*, RSC, 2012, ch. 9, pp. 317-349; (d) O. S. Wenger, *Chem. Soc. Rev.*, 2012, **41**, 3772-3779; (e) M. Akita, *Organometallics*, 2011, **30**, 43-51; (f) V. Guerchais, L. Ordronneau and H. L. Bozec, *Coord. Chem. Rev.*, 2010, **254**, 2533-2545; (g) C.-C. Ko and V. W.-W. Yam, *J. Mater. Chem.*, 2010, **20**, 2063-2070; (h) V. Guerchais and H. Le Bozec, in *Molecular Organometallic Materials for Optics*, eds. H. Bozec and V. Guerchais, Springer Berlin Heidelberg, Berlin, Heidelberg, 2010, pp. 171-225; (i) P. Belser, L. De Cola, F. Hartl, V. Adamo, B. Bozic, Y. Chriqui, V. M. Iyer, R. T. F. Jukes, J. Kuhni, M. Querol, S. Roma and N. Salluce, *Adv. Funct. Mat.*, 2006, **16**, 195-208.
63. (a) S. Kume, M. Kurihara and H. Nishihara, *J. Korean Electrochem. Soc.*, 2002, **5**, 189-191; (b) S. Kume, M. Kurihara and H. Nishihara, *Inorg. Chem.*, 2003, **42**, 2194-2196; (c) S. Umeki, S. Kume and H. Nishihara, *Chem. Lett.*, 2010, **39**, 204-205; (d) S. Umeki, S. Kume and H. Nishihara, *Inorg. Chem.*, 2011, **50**, 4925-4933; (e) S. Kume, M. Murata, T. Ozeki and H. Nishihara, *J. Am. Chem. Soc.*, 2005, **127**, 490-491; (f) R. Sakamoto, S. Kume, M. Sugimoto and H. Nishihara, *Chem. Eur. J.*, 2009, **15**, 1429-1439; (g) S. Kume, M. Kurihara and H. Nishihara, *Chem. Commun.*, 2001, 1656-1657; (h) R. Sakamoto, M. Murata, S. Kume, H. Sampei, M. Sugimoto and H. Nishihara, *Chem. Commun.*, 2005, 1215-1217; (i) K. Yamaguchi, S. Kume, K. Namiki, M. Murata, N. Tamai and H. Nishihara, *Inorg. Chem.*, 2005, **44**, 9056-9067; (j) H. Nishihara, *Coord. Chem. Rev.*, 2005, **249**, 1468-1475; (k) J. Otsuki, N. Omokawa, K. Yoshiba, I. Yoshikawa, T. Akasaka, T. Suenobu, T. Takido, K. Araki and S. Fukuzumi, *Inorg. Chem.*, 2003, **42**, 3057-3066; (l) A. Telleria, J. Pérez-Miqueo, A. Altube, E. García-Lecina, A. de Cózar and Z. Freixa, *Organometallics*, 2015, **34**, 5513-5529.
64. (a) J. Pérez-Miqueo, A. Altube, E. García-Lecina, A. Tron, N. D. McClenaghan and Z. Freixa, *Dalton Trans.*, 2016, **45**, 13726-13741; (b) J. Pérez-Miqueo, A. Telleria, M. Muñoz-Olasagasti, A. Altube, E. García-Lecina, A. de Cózar and Z. Freixa, *Dalton Trans.*, 2015, **44**, 2075-2091; (c) J. Pérez-Miqueo, PhD thesis, University of the Basque Country (UPV-EHU), 2017.
65. M. Kaiser, S. P. Leitner, C. Hirtenlehner, M. List, A. Gerisch and U. Monkowius, *Dalton Trans.*, 2013, **42**, 14749-14756.
66. (a) S. Thies, H. Sell, C. Bornholdt, C. Schütt, F. Köhler, F. Tuczek and R. Herges, *Chem. Eur. J*, 2012, **18**, 16358-16368; (b) S. Thies, H. Sell, C. Schütt, C. Bornholdt, C. Näther, F. Tuczek and R. Herges, *J. Am. Chem. Soc*, 2011, **133**, 16243-16250; (c) C. Schütt, G. Heitmann, T. Wendler, B. Krahwinkel and R. Herges, *J. Org. Chem.*, 2016, **81**, 1206-1215.
67. (a) K. Suwa, J. Otsuki and K. Goto, *Tetrahedron Lett.*, 2009, **50**, 2106-2108; (b) K. Suwa, J. Otsuki and K. Goto, *J. Phys. Chem. A*, 2010, **114**, 884-890.
68. E. C. Harvey, B. L. Feringa, J. G. Vos, W. R. Browne and M. T. Pryce, *Coord. Chem. Rev.*, 2015, **282-283**, 77-86.
69. G. Bianchini, G. Strukul, D. F. Wass and A. Scarso, *RSC Adv.*, 2015, **5**, 10795-10798.
70. (a) T. Koike and M. Akita, in *New Frontiers in Photochromism*, eds. M. Irie, Y. Yokoyama and T. Seki, Springer Japan, Tokyo, 2013, pp. 205-224; (b) R. T. F. Jukes, V. Adamo, F. Hartl, P. Belser and L. De Cola, *Inorg. Chem.*, 2004, **43**, 2779-2792; (c) R. T. F. Jukes, V. Adamo, F. Hartl, P. Belser and L. De Cola, *Coord. Chem. Rev.*, 2005, **249**, 1327-1335; (d) S. Fraysse, C. Coudret and J.-P. Launay, *Eur. J. Inorg. Chem.*, 2000, **2000**, 1581-1590; (e) Y. Tanaka, T. Ishisaka, A. Inagaki, T. Koike, C. Lapinte and M. Akita, *Chem. Eur. J*, 2010, **16**, 4762-4776; (f) K. Uchida, A. Inagaki and M. Akita, *Organometallics*, 2007, **26**, 5030-5041; (g) G. Cosquer, M. Kamila, Z.-Y. Li, K. B. Breedlove and M. Yamashita, *Inorganics*, 2018, **6**, 9; (h) M. Giraud, A. Léaustic, R. Guillot, P. Yu, P. Dorlet, R. Métivier and K. Nakatani, *New J. Chem.*, 2009, **33**, 1380-1385.
71. (a) M. Querol, H. Stoekli-Evans and P. Belser, *Org. Lett.*, 2002, **4**, 1067-1070; (b) S. J. Wezenberg, K.-Y. Chen and B. L. Feringa, *Angew. Chem. Int. Ed.*, 2015, **54**, 11457-11461; (c) A. Faulkner, T. van Leeuwen, B. L. Feringa and S. J. Wezenberg, *J. Am. Chem. Soc.*, 2016, **138**, 13597-13603.
72. D. Astruc, *Organometallic Chemistry and Catalysis*, Springer, 2007.